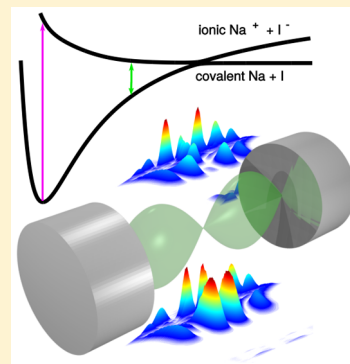


Cavity Femtochemistry: Manipulating Nonadiabatic Dynamics at Avoided Crossings

Markus Kowalewski,* Kochise Bennett, and Shaul Mukamel*

Chemistry Department, University of California, Irvine, California 92697-2025, United States

ABSTRACT: Molecular potential energy surfaces can be actively manipulated by light. This is usually done by strong classical laser light but was recently demonstrated for the quantum field in an optical cavity. The photonic vacuum state of a localized cavity mode can be strongly mixed with the molecular degrees of freedom to create hybrid field-matter states known as polaritons. We simulate the avoided crossing of sodium iodide in a cavity by incorporating the quantized cavity field into the nuclear wave packet dynamics calculation. The quantized field is represented on a numerical grid in quadrature space, thus avoiding the limitations set by the rotating wave approximation (RWA) when the field is expanded in Fock space. This approach allows the investigation of cavity couplings in the vicinity of naturally occurring avoided crossings and conical intersections, which is too expensive in the fock space expansion when the RWA does not apply. Numerical results show how the branching ratio between the covalent and ionic dissociation channels can be strongly manipulated by the optical cavity.



The photochemistry of molecules can be significantly influenced by specially tailored electromagnetic fields.^{1–7} While control is usually achieved with classical laser fields, a strong coupling with the vacuum state of a cavity utilizes the quantum nature of the electromagnetic mode. The underlying theoretical framework, cavity quantum electrodynamics, has been well developed in theory and experiment for atoms^{8–11} and has been applied to atomic trapping and cooling.¹² Its potential applications to molecular cooling,^{13,14} as a tool to probe larger molecules,^{15,16} to enhance vibrational spectra,^{17–20} for use with electromagnetically induced transparency,²¹ and to expedite cavity-modified photochemistry^{22,23} have been objects of intensive studies. Strong cavity coupling in molecular systems has been demonstrated recently for electronic transitions²⁴ and for vibrational transitions.^{18,25} In this regime, the dynamics is described using joint photon-matter states called polaritons. The inclusion of the internal nuclear degrees of freedom, not present in atoms, gives rise to nonadiabatic dynamics.^{23,26} The light field can strongly mix the nuclear and electronic degrees of freedom, creating avoided curve crossings and conical intersections (CIs) between the polariton potential energy surfaces. Virtually all photochemical and photophysical processes are controlled by the presence of naturally occurring CIs in the bare electronic energy landscape, opening up fast, nonradiative relaxation pathways by which the molecule is funneled back to the ground state.

In this contribution, we theoretically investigate how a molecule that already possesses a curve crossing is affected by strong coupling to a nanoscale cavity. To set the stage, we first neglect the nuclear degrees of freedom and only introduce them at a later point. This will allow us to introduce the basic structure of the Hamiltonian and the cavity coupling. The Hamiltonian describing the light-matter interaction of a two-

level system linearly coupled to a quantized radiation field is given by the quantum Rabi model²⁷

$$\hat{H}_{ec} = H_e + H_c + H_I$$

$$= \frac{\hbar\omega_0}{2}(2\hat{\sigma}^\dagger\hat{\sigma} - 1) + \hbar\omega_c\hat{a}^\dagger\hat{a} + \hbar g(\hat{a}^\dagger + \hat{a})(\hat{\sigma}^\dagger + \hat{\sigma}) \quad (1)$$

where $\hbar\omega_0 = \hbar(\omega_e - \omega_g)$ is the energy difference between the excited state $|e\rangle$ and the ground state $|g\rangle$, $\hat{\sigma} = |g\rangle\langle e|$ is the annihilation operator for the bare electronic excitation, and $\hat{a}^{(\dagger)}$ annihilates (creates) a cavity photon of mode frequency ω_c . The vacuum Rabi-frequency $g = \sqrt{n}\mu_{eg}\epsilon_c/\hbar$, the coupling between the photon mode and the electronic degrees of freedom, depends on the electronic transition dipole moment μ_{eg} and the vacuum field amplitude

$$\epsilon_c = \sqrt{\frac{\hbar\omega_c}{V\epsilon_0}} \quad (2)$$

This amplitude is determined by the active volume V of the cavity mode. Nanoscale cavities can thus induce very strong coupling. The cavity coupling is further enhanced by a factor of \sqrt{n} if an ensemble of n molecules contributes in a coherent fashion in a cavity smaller than the optical wavelength $2\pi c/\omega_c$.

Different approximations can be used to find the eigenvalues of eq 1 depending on the magnitude of g . Perturbative solutions are possible when g is much smaller than all other system frequencies. If the time scale g^{-1} is faster than possible decay processes, we enter the strong coupling regime though the

Received: April 21, 2016

Accepted: May 17, 2016

counter rotating terms ($a\sigma$ and $a^\dagger\sigma^\dagger$) in the Hamiltonian can be neglected. This is known as the Jaynes-Cummings (JC) model⁹ and approximates solutions to the Hamiltonian (eq 1) in the form of dressed states, which are then expressed in the basis of the photon number states:

$$\Psi_c = \sum_{n=0}^M c_{g,n}|g, n_c\rangle + c_{e,n}|e, n_c\rangle \quad (3)$$

Here n_c is the number of photons in the cavity mode, and M is total number of photon number states. The JC model keeps only the $a\sigma^\dagger$ and $a^\dagger\sigma$ terms in the cavity-molecule coupling. The total matter+field excitation number, $\hat{N} \equiv \hat{n}_c + \hat{\sigma}^\dagger\hat{\sigma}$, is a conserved quantity ($[\hat{N}, \hat{H}] = 0$), reducing the Hamiltonian to a 2-by-2 block-diagonal form (see Figure 1). Assuming that the

$$\begin{pmatrix} N_0 & & (a\sigma) & & \\ & \left(N_1 \right) & & & \ddots \\ (a^\dagger\sigma^\dagger) & & \left(N_2 \right) & & \\ & \ddots & & \ddots & \ddots \end{pmatrix}$$

Figure 1. Atom-field Hamiltonian for quantum Rabi problem. The resonant coupling terms $\sigma^\dagger a$ and σa^\dagger act within each block N_1, \dots, N_M . The non-RWA terms $a\sigma$ and $a^\dagger\sigma^\dagger$ couple different blocks.

cavity is initially in the vacuum state (no photons), the wave function in the JC model can thus be expressed by the two dressed states $|g, 1\rangle, |e, 0\rangle$ and the ground state $|g, 0\rangle$, i.e., the bare ground state with 1 photon and the excited state with 0 photons. An extension of the JC model to include the nuclear degrees of freedom within the RWA has been presented recently.²³ However, when the RWA is violated, the expansion (eq 3) requires a large number of Fock states to converge, becoming intractable for quantum dynamics time propagation (scaling with $O(M^2)$).

To overcome this difficulty we employ an efficient computational scheme obtained by the direct treatment of the cavity mode as a quantum harmonic oscillator in quadrature space. We first express the annihilation and creation operators of the cavity mode in terms of their quadrature coordinates x and p :²⁷

$$a = \sqrt{\frac{\omega_c}{2\hbar}} \left(\hat{x} + \frac{i}{\omega_c} \hat{p} \right) \quad (4)$$

with $p = -i\hbar\partial_x$. The extension of the Hamiltonian to the molecular case is now straightforward: The nuclear degrees of freedom $q \equiv (q_1, \dots, q_N)$ are accounted for by treating ω_0 and g as functions of q (i.e., the potential energy curves $V_g \equiv V_g(q)$, $V_e \equiv V_e(q)$, and the transition dipole curves $\mu_{eg} \equiv \mu_{eg}(q)$ respectively). The coupled light-molecule Hamiltonian eq 1 then reads:

$$H_{ec} = \frac{\omega_0(q)}{2} (2\hat{\sigma}^\dagger\hat{\sigma} - 1) - \frac{\hbar}{2} \frac{\partial^2}{\partial x^2} + \frac{1}{2} \omega_c^2 \hat{x}^2 + g(q) \sqrt{2\hbar\omega_c} \hat{x} (\hat{\sigma}^\dagger + \hat{\sigma}) \quad (5)$$

The total wave function expanded in the adiabatic electronic states $|\phi_g\rangle$ and $|\phi_e\rangle$ becomes

$$\Psi = \psi_g(x, q)|\phi_g\rangle + \psi_e(x, q)|\phi_e\rangle \quad (6)$$

Note that the wave function of the cavity mode and the nuclear degrees of freedom are generally nonseparable ($\psi_k(x, q)$). The matrix elements of the cavity-molecule Hamiltonian in the basis of the bare adiabatic states are then

$$H_{kl} = \delta_{kl} \left(\hat{T}_{\text{nuc}} + \hat{V}_k - \frac{\hbar}{2} \frac{\partial^2}{\partial x^2} + \frac{1}{2} \omega_c^2 \hat{x}^2 \right) + (1 - \delta_{kl}) g \sqrt{2\hbar\omega_c} \hat{x} \quad (7)$$

where

$$\hat{T}_{\text{nuc}} = -\frac{\hbar}{2} \sum_i \frac{1}{m_i} \frac{\partial^2}{\partial q_i^2} \quad (8)$$

is the nuclear kinetic energy operator, m_i the reduced mass of the vibrational mode q_i , and $\delta_{kl} = 1$ if $k = l$ and zero otherwise. The indices k and l run over the bare electronic states g and e . The coordinate x is expanded in a numerical grid, putting the nuclear coordinates and the cavity mode on an equal footing in a numerical simulation. The second derivative with respect to x can be conveniently calculated by a discrete Fourier transform.²⁸ For a diatomic molecule, this results in two-dimensional potential energy surfaces for the electronic ground and excited state, each depending on q and x . This yields a more favorable scaling of the computational effort of $O(n \log n)$ rather than $O(n^2)$ in the basis of photon number states. For the case of large cavity coupling, the number of grid points in x necessary is in practice even smaller than the number of Fock states.²⁹

The effect of ultrastrong cavity coupling on nonadiabatic dynamics is demonstrated on the excited state dynamics of sodium iodide, which has been an important landmark in femtochemistry.³¹ The adiabatic electronic states of the bare sodium iodide experience an avoided crossing near $q \sim 8 \text{ \AA}$ (Figure 2a), which leads to dissociation into the neutral products through the 1X state. Upon photoexcitation, a nuclear wave packet is launched in the 1A state and then oscillates back and forth.³² Part of the wave packet couples to the 1X state via the avoided crossing into the covalent dissociation channel. The corresponding nonadiabatic coupling matrix element, responsible for the population transfer between the 1A and the 1X state, is shown in Figure 2b (red curve). The branching ratio, i.e., the population transferred to the 1X state, is determined by the momentum of the wave packet, which in turn depends on the wavelength of the pump laser. Zewail had measured a stepwise increase in the covalent state population of $\approx 11\%$ at each passage through the avoided crossing.³² To influence the dynamics at the avoided crossing, the cavity needs to be set in resonance with the 1X and the 1A state in a region where the transition dipole moment is significantly large ($\approx 2-9 \text{ \AA}$; see Figure 2b, blue curve). We will investigate the scenario where the cavity is set in resonance at $\approx 6 \text{ \AA}$, i.e., before the wave packet in the 1A state reaches the avoided crossing ($\hbar\omega_c = 815 \text{ meV}$).

Wave packet calculations were carried out to reveal the possible modifications of the dynamics under the influence of the cavity coupling. This was done by propagating the photonic-nuclear wave packet with a Chebychev propagation scheme³³ on the potential energy curves of NaI (1X and 1A) using the Hamiltonian from eq 7 and an additional coupling term^{34,35} to account for the nonadiabatic coupling at the bare state avoided crossing:

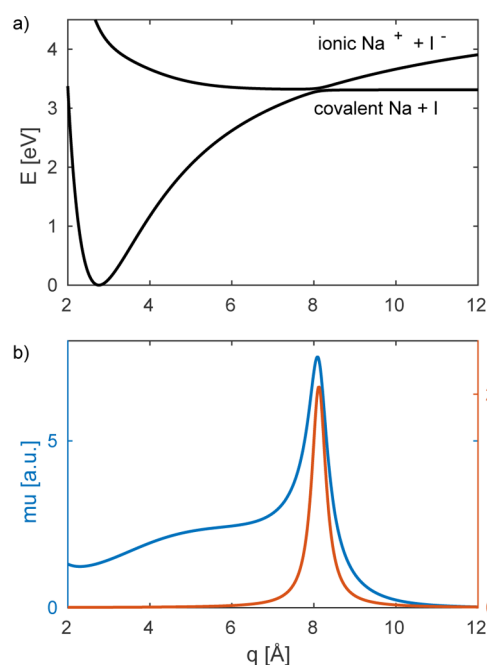


Figure 2. (a) Bare ground (¹X) and excited (¹A) electronic potential energy surfaces of NaI. Dissociation on the ¹X potential leads to the neutral reaction products. (b) Transition dipole moment μ_{eg} (blue) and the derivative coupling matrix element f_{eg} (red). The potential energy curves, the nonadiabatic coupling matrix element, and the transition dipole moment were calculated with the program package MOLPRO³⁰ at the MRCI/CAS(6/7)/aug-cc-VQZ level of theory with an effective core potential for Iodine (ECP46MWB).

$$\hat{H}_{kl}^{\text{nac}} = \hat{H}_{kl} + (1 - \delta_{kl}) \frac{\hbar}{2m} (2f_{kl} \partial_q + \partial_q f_{kl}) \quad (9)$$

where f_{kl} is the nonadiabatic coupling matrix element shown in Figure 2b. The wave function, as well as the potential energy surfaces, are represented by a numerical grid with 95 points for x and 1200 points for q . The initial condition is a product state formed by the vacuum state of the cavity $|0\rangle$ and the vibrational ground state of the ¹X state $|^1X, \nu = 0\rangle$ shifted by 0.63 Å.

Figure 3a shows the time-dependent population of the covalent state of the free molecule (no cavity), mimicking the original experimental setup.³² The dynamics of the system is presented by inspecting the time evolution of the population of the ¹X state, $\langle \psi_X | \psi_X \rangle$, rather than the pump–probe signal, which probes the excited state wave packet within a certain window of internuclear distance. The stepwise decay observed in the pump–probe experiment (e.g., ref 32, Figure 8) is less clear for the total population but it better illustrates the overall effect of the cavity. In Figure 3b, the time evolution in a cavity is shown for moderate coupling strength ($g = (0.05, 0.13)\omega_c$). The time traces are still similar to the uncoupled case but already show the influence of the cavity coupling. At coupling strengths of $g \approx 0.19\omega_c$ (Figure 3c), the behavior of the time traces begins to change. The dissociation is suppressed, and the oscillation period increases. The wave packet becomes trapped in a more tight effective potential, and its recurrence time becomes shorter. The dynamics is mainly influenced by two modifications of the potential energy surfaces: the new avoided crossing created by the cavity and the modified avoided crossing already present in the bare molecule. With increased cavity coupling, the cavity-created crossing generates well-separated states such that a nuclear wave packet is trapped, and

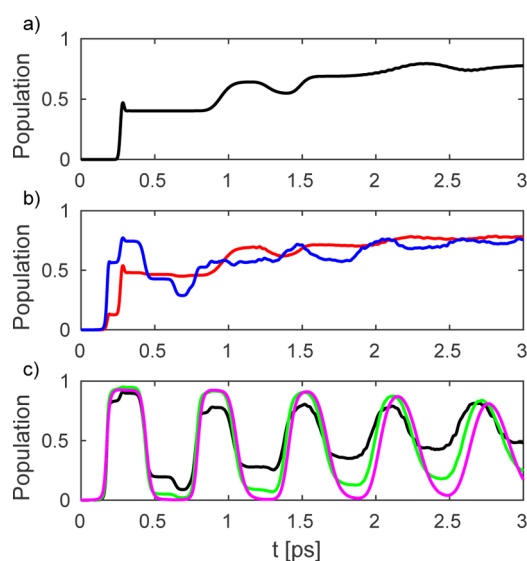


Figure 3. Selected time traces of the ¹X state population following impulsive excitation. (a) No cavity. (b) $g = 0.050\omega_c$ (red), $g = 0.13\omega_c$ (blue). (c) $g = 0.19\omega_c$ (black), $g = 0.25\omega_c$ (green), $g = 0.38\omega_c$ (magenta).

a much smaller fraction reaches the original crossing. This partially coincides with the effect described by Galego et al.²⁶ for higher coupling strengths, the states become well separated and the Born–Oppenheimer approximation regains validity. For larger splittings, the upper polariton state is well separated from the lower lying states, effectively suppressing the nonadiabatic population transfer. Moreover, the nonadiabatic coupling at the original intersection is affected by the off-resonant interaction with the cavity allowing for further suppression of the population transfer into the covalent channel. For higher coupling strengths, the dissociation is strongly suppressed.

The scaling of the dynamics with g can be displayed in terms of the population in the ¹X state after the wave packet has reached the crossing point for the first time (≈ 480 fs). Figure 4a depicts the population in the covalent channel for varying coupling strengths. While an intermediate coupling strength ($g < 0.1\omega_c$) can slightly increase the dissociation probability, the transfer to the ¹X state is suppressed for larger values of g .

We have employed an efficient computational protocol for cavity nonadiabatic dynamics, which allows for a seamless integration of quantized field modes into existing schemes at a cost comparable to adding another vibrational mode to the system. The Hamiltonian used to calculate the dynamics (eq 7) is in a very general form and can be used for a wide range of cavity couplings. It only relies on the dipole approximation, making it robust and reliable. We have demonstrated the method for an avoided crossing and one vibrational mode, but it can be applied to more than one vibrational mode, which will allow addressing conical intersections. Including additional cavity modes is also straightforward and only limited by its computational cost. While a partially analytic solution of the non-RWA problem based on tunable coherent states is possible³⁶ and might give insight into the resulting structure of the diagonalized potential energy surfaces, it might become intractable for a quantum dynamics time propagation.

Our wave packet simulations show that the photochemistry of NaI can be significantly manipulated by the cavity. This is caused by two mechanisms: in the strong coupling regime, the

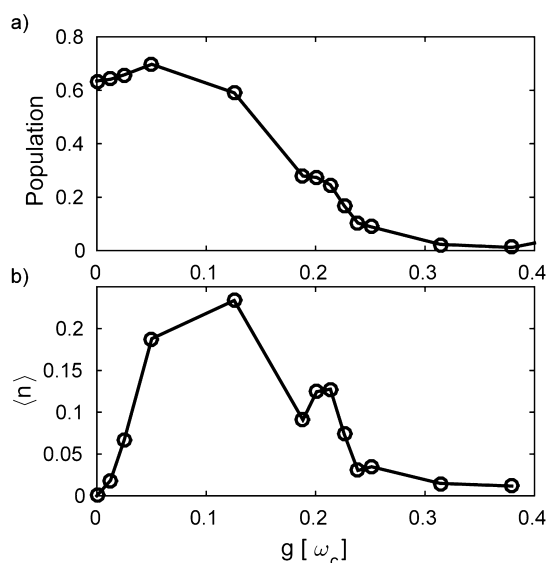


Figure 4. (a) Population of the covalent state after 480 fs vs the cavity coupling strength. (b) corresponding average photon numbers.

modification of the 1A state becomes significant and a new avoided crossing is created, introducing a new turning point for the wave packet motion. When the coupling strength enters the ultrastrong coupling regime, the 1X ground state is strongly modified in the region of the bare state avoided crossing. To reach this regime, effective cavity volumes (eq 2) on the order of the optical wavelength or less are necessary along with a collective enhancement. For the example shown in Figure 3, and under the assumption of typical particle numbers³⁷ of 10^5 , the effective cavity volume range from $0.002 \lambda_c^3$ to $0.04 \lambda_c^3$, where λ_c is the wavelength of the cavity mode. Such small volumes could potentially be realized by, e.g., nano cavities,^{38,39} nano plasmon antennas,⁴⁰ or nano guides.⁴¹ The collective enhancement of the coupling in molecular systems, however, is subject to dephasing and needs further investigation.

AUTHOR INFORMATION

Corresponding Authors

*E-mail: mkowalew@uci.edu.

*E-mail: smukamel@uci.edu.

Notes

The authors declare no competing financial interest.

ACKNOWLEDGMENTS

The support of the National Science Foundation (Grant CHE-1361516) and the support from the Chemical Sciences, Geosciences, and Biosciences division, Office of Basic Energy Sciences, Office of Science, U.S. Department of Energy, through award No. DE-FG02-04ER15571 is gratefully acknowledged. K.B. was supported by the DOE. M.K. gratefully acknowledges support from the Alexander von Humboldt foundation through the Feodor Lynen program. We would like to thank the green planet cluster (NSF Grant CHE-0840513) for allocation of compute resources.

REFERENCES

- Demekhin, P. V.; Cederbaum, L. S. Light-induced conical intersections in polyatomic molecules: General theory, strategies of exploitation, and application. *J. Chem. Phys.* **2013**, *139*, 154314.
- Kim, J.; Tao, H.; White, J. L.; Petrović, V. S.; Martinez, T. J.; Bucksbaum, P. H. Control of 1,3-Cyclohexadiene Photoisomerization Using Light-Induced Conical Intersections. *J. Phys. Chem. A* **2012**, *116*, 2758–2763.
- von den Hoff, P.; Kowalewski, M.; de Vivie-Riedle, R. Searching for pathways involving dressed states in optimal control theory. *Faraday Discuss.* **2011**, *153*, 159–171.
- von den Hoff, P.; Thallmair, S.; Kowalewski, M.; Siemering, R.; de Vivie-Riedle, R. Optimal control theory - closing the gap between theory and experiment. *Phys. Chem. Chem. Phys.* **2012**, *14*, 14460–14485.
- Gross, P.; Neuhauser, D.; Rabitz, H. Optimal control of curve-crossing systems. *J. Chem. Phys.* **1992**, *96*, 2834–2845.
- Brumer, P.; Shapiro, M. Control of unimolecular reactions using coherent light. *Chem. Phys. Lett.* **1986**, *126*, 541–546.
- Tannor, D. J.; Kosloff, R.; Rice, S. A. Coherent pulse sequence induced control of selectivity of reactions: Exact quantum mechanical calculations. *J. Chem. Phys.* **1986**, *85*, 5805–5820.
- Purcell, E. M. Spontaneous Emission Probabilities at Radio Frequencies. *Phys. Rev.* **1946**, *69*, 674.
- Jaynes, E. T.; Cummings, F. W. Comparison of quantum and semiclassical radiation theories with application to the beam maser. *Proc. IEEE* **1963**, *51*, 89–109.
- Haroche, S.; Raimond, J.-M. *Exploring the Quantum: Atoms, Cavities, and Photons (Oxford Graduate Texts)*, 1st ed.; Oxford University Press: Oxford, U.K., 2006.
- Haroche, S. Nobel Lecture: Controlling photons in a box and exploring the quantum to classical boundary. *Rev. Mod. Phys.* **2013**, *85*, 1083–1102.
- Nuszmann, S.; Murr, K.; Hijlkema, M.; Weber, B.; Kuhn, A.; Rempe, G. Vacuum-stimulated cooling of single atoms in three dimensions. *Nat. Phys.* **2005**, *1*, 122–125.
- Kowalewski, M.; Morigi, G.; Pinkse, P. W. H.; de Vivie Riedle, R. Cavity sideband cooling of trapped molecules. *Phys. Rev. A: At., Mol., Opt. Phys.* **2011**, *84*, 033408.
- Lev, B. L.; Vukics, A.; Hudson, E. R.; Sawyer, B. C.; Domokos, P.; Ritsch, H.; Ye, J. Prospects for the cavity-assisted laser cooling of molecules. *Phys. Rev. A: At., Mol., Opt. Phys.* **2008**, *77*, 023402.
- Spano, F. C. Optical microcavities enhance the exciton coherence length and eliminate vibronic coupling in J-aggregates. *J. Chem. Phys.* **2015**, *142*, 184707.
- Caruso, F.; Saikin, S. K.; Solano, E.; Huelga, S. F.; Guzik, A. A.; Plenio, M. B. Probing biological light-harvesting phenomena by optical cavities. *Phys. Rev. B: Condens. Matter Mater. Phys.* **2012**, *85*, 125424.
- Saurabh, P.; Mukamel, S. Two-dimensional infrared spectroscopy of vibrational polaritons of molecules in an optical cavity. *J. Chem. Phys.* **2016**, *144*, 124115.
- Shalabney, A.; George, J.; Hiura, H.; Hutchison, J. A.; Genet, C.; Hellwig, P.; Ebbesen, T. W. Enhanced Raman Scattering from Vibro-Polariton Hybrid States. *Angew. Chem., Int. Ed.* **2015**, *54*, 7971–7975.
- del Pino, J.; Feist, J.; Garcia-Vidal, F. J. Signatures of Vibrational Strong Coupling in Raman Scattering. *J. Phys. Chem. C* **2015**, *119*, 29132–29137.
- Simpkins, B. S.; Fears, K. P.; Dressick, W. J.; Spann, B. T.; Dunkelberger, A. D.; Owrutsky, J. C. Spanning Strong to Weak Normal Mode Coupling between Vibrational and Fabry-Pérot Cavity Modes through Tuning of Vibrational Absorption Strength. *ACS Photonics* **2015**, *2*, 1460–1467.
- Herrera, F.; Peropadre, B.; Pachon, L. A.; Saikin, S. K.; Aspuru-Guzik, A. Quantum Nonlinear Optics with Polar J-Aggregates in Microcavities. *J. Phys. Chem. Lett.* **2014**, *5*, 3708–3715.
- Herrera, F.; Spano, F. C. Cavity-controlled chemistry in molecular ensembles. 2015; <http://arxiv.org/abs/1512.05017> (accessed May 12, 2016).
- Kowalewski, M.; Bennett, K.; Mukamel, S. Non-adiabatic dynamics of molecules in optical cavities. *J. Chem. Phys.* **2016**, *144*, 054309.

- (24) Hutchison, J. A.; Schwartz, T.; Genet, C.; Devaux, E.; Ebbesen, T. W. Modifying Chemical Landscapes by Coupling to Vacuum Fields. *Angew. Chem., Int. Ed.* **2012**, *51*, 1592–1596.
- (25) Muallem, M.; Palatnik, A.; Nessim, G. D.; Tischler, Y. R. Strong Light-Matter Coupling and Hybridization of Molecular Vibrations in a Low-Loss Infrared Microcavity. *J. Phys. Chem. Lett.* **2016**, 2002. (just accepted manuscript).
- (26) Galego, J.; Garcia-Vidal, F. J.; Feist, J. Cavity-Induced Modifications of Molecular Structure in the Strong-Coupling Regime. *Phys. Rev. X* **2015**, *5*, 041022.
- (27) Schleich, W. P. *Quantum Optics in Phase Space*, 1st ed.; Wiley-VCH: Berlin, 2001.
- (28) Tannor, D. J. *Introduction to Quantum Mechanics: A Time-Dependent Perspective*; University Science Books: Sausalito, CA, 2006.
- (29) Chen, Q.-H.; Wang, C.; He, S.; Liu, T.; Wang, K.-L. Exact solvability of the quantum Rabi model using Bogoliubov operators. *Phys. Rev. A: At., Mol., Opt. Phys.* **2012**, *86*, 023822.
- (30) Werner, H.-J.; Knowles, P. J.; Knizia, G.; Manby, F. R.; Schütz, M., et al. MOLPRO, version 2015.1, a package of ab initio programs. 2015; see <http://www.molpro.net> (accessed May 11, 2016).
- (31) Mokhtari, A.; Cong, P.; Herek, J. L.; Zewail, A. H. Direct femtosecond mapping of trajectories in a chemical reaction. *Nature* **1990**, *348*, 225–227.
- (32) Rose, T. S.; Rosker, M. J.; Zewail, A. H. Femtosecond realtime probing of reactions. IV. The reactions of alkali halides. *J. Chem. Phys.* **1989**, *91*, 7415–7436.
- (33) Tal-Ezer, H.; Kosloff, R. An accurate and efficient scheme for propagating the time dependent Schrödinger equation. *J. Chem. Phys.* **1984**, *81*, 3967–3971.
- (34) Hofmann, A.; de Vivie-Riedle, R. Adiabatic approach for ultrafast quantum dynamics mediated by simultaneously active conical intersections. *Chem. Phys. Lett.* **2001**, *346*, 299–304.
- (35) Domcke, W.; Yarkony, D. R.; Köppel, H. *Conical Intersections*; World Scientific: Singapore, 2011; Vol. 17.
- (36) Chen, Q.-H.; Liu, T.; Zhang, Y.-Y.; Wang, K.-L. Exact solutions to the Jaynes-Cummings model without the rotating-wave approximation. *Europhys. Lett.* **2011**, *96*, 14003.
- (37) Schwartz, T.; Hutchison, J. A.; Léonard, J.; Genet, C.; Haacke, S.; Ebbesen, T. W. Polariton Dynamics under Strong Light-Molecule Coupling. *ChemPhysChem* **2013**, *14*, 125–131.
- (38) Tomljenovic-Hanic, S.; Steel, M. J.; de Sterke, C. M.; Salzman, J. Diamond based photonic crystal microcavities. *Opt. Express* **2006**, *14*, 3556–3562.
- (39) Greentree, A. D.; Tahan, C.; Cole, J. H.; Hollenberg, L. C. L. Quantum phase transitions of light. *Nat. Phys.* **2006**, *2*, 856–861.
- (40) Kim, M.-K.; Sim, H.; Yoon, S. J.; Gong, S.-H.; Ahn, C. W.; Cho, Y.-H.; Lee, Y.-H. Squeezing Photons into a Point-Like Space. *Nano Lett.* **2015**, *15*, 4102–4107.
- (41) Faez, S.; Türschmann, P.; Haakh, H. R.; Göttinger, S.; Sandoghdar, V. Coherent Interaction of Light and Single Molecules in a Dielectric Nanoguide. *Phys. Rev. Lett.* **2014**, *113*, 213601.